




RESEARCH ARTICLE

Structural brain network lateralization across childhood and adolescence

Brandon T. Craig^{1,2,3}  | Bryce Geeraert^{1,2} | Eli Kinney-Lang^{1,2} |
Alicia J. Hilderley^{1,2} | Keith O. Yeates^{1,2,4} | Adam Kirton^{1,2,3,5,6} |
Melanie Noel^{1,2,4} | Frank P. MacMaster^{1,2,7,8,9} | Signe Bray^{1,2,6,8} |
Karen M. Barlow^{1,2,8,10} | Brian L. Brooks^{1,2,3,4,5} | Catherine Lebel^{1,2,6,8}  |
Helen L. Carlson^{1,2,3} 

¹University of Calgary, Alberta Children's Hospital Research Institute, Calgary, Alberta, Canada

²University of Calgary, Hotchkiss Brain Institute, Calgary, Alberta, Canada

³Department of Pediatrics, University of Calgary, Calgary, Alberta, Canada

⁴Department of Psychology, University of Calgary, Calgary, Alberta, Canada

⁵Department of Clinical Neurosciences, University of Calgary, Calgary, Alberta, Canada

⁶Department of Radiology, University of Calgary, Calgary, Alberta, Canada

⁷Department of Psychiatry, University of Calgary, Calgary, Alberta, Canada

⁸Child and Adolescent Imaging Research (CAIR) Program, Cumming School of Medicine, University of Calgary, Calgary, Alberta, Canada

⁹Strategic Clinical Network for Addictions and Mental Health, Alberta Health Services, Calgary, Alberta, Canada

¹⁰Child Health Research Centre, The University of Queensland, Brisbane, Queensland, Australia

Correspondence

Helen L. Carlson, Alberta Children's Hospital Research Institute, 28 Oki Drive NW, Calgary, AB T3B 6A8, Canada.
Email: helen.carlson@albertahealthservices.ca

Funding information

Alberta Children's Hospital Foundation; Alberta Health Services; Canadian Institute of Health Research (CIHR) Embedded Clinician Researcher Salary Award; Vanier Canadian Graduate Scholarship

Abstract

Developmental lateralization of brain function is imperative for behavioral specialization, yet few studies have investigated differences between hemispheres in structural connectivity patterns, especially over the course of development. The present study compares the lateralization of structural connectivity patterns, or topology, across children, adolescents, and young adults. We applied a graph theory approach to quantify key topological metrics in each hemisphere including efficiency of information transfer between regions (global efficiency), clustering of connections between regions (clustering coefficient [CC]), presence of hub-nodes (betweenness centrality [BC]), and connectivity between nodes of high and low complexity (hierarchical complexity [HC]) and investigated changes in these metrics during development. Further, we investigated BC and CC in seven functionally defined networks. Our cross-sectional study consisted of 211 participants between the ages of 6 and 21 years with 93% being right-handed and 51% female. Global efficiency, HC, and CC demonstrated a leftward lateralization, compared to a rightward lateralization of BC. The sensorimotor, default mode, salience, and language networks showed a leftward

This is an open access article under the terms of the [Creative Commons Attribution-NonCommercial-NoDerivs](https://creativecommons.org/licenses/by-nc-nd/4.0/) License, which permits use and distribution in any medium, provided the original work is properly cited, the use is non-commercial and no modifications or adaptations are made.

© 2022 The Authors. *Human Brain Mapping* published by Wiley Periodicals LLC.

asymmetry of CC. BC was only lateralized in the salience (right lateralized) and dorsal attention (left lateralized) networks. Only a small number of metrics were associated with age, suggesting that topological organization may stay relatively constant throughout school-age development, despite known underlying changes in white matter properties. Unlike many other imaging biomarkers of brain development, our study suggests topological lateralization is consistent across age, highlighting potential nonlinear mechanisms underlying developmental specialization.

KEYWORDS

lateralization, structural connectome, typical brain development

1 | INTRODUCTION

The lateralization of brain functions has been of interest since Broca's seminal finding that speech production is largely isolated to the left hemisphere (Broca, 1861). Numerous functions have subsequently been shown to be strongly lateralized, such as spatial awareness, where right posterior parietal cortex lesions may lead to hemispatial neglect (Stone et al., 1991; Wernicke, 1874). Although macrostructure appears similar in both hemispheres, we now know that cellular and functional mechanisms differ between the left and right hemispheres and in turn play different roles in neurological function (Toga & Thompson, 2003). Therefore, an understanding of how the brain's lateralization of function develops in a typically developing population may be informative for discerning different trajectories in those with atypical neurological outcomes.

There are numerous ways to investigate brain laterality and development. However, over the last few decades, neuroimaging has become the gold-standard of assessing brain laterality and development. Such techniques have revealed macro-level structural changes in brain lateralization across development showing asymmetries in gray matter (Zhou et al., 2013) and white matter. More advanced neuroimaging techniques, such as diffusion magnetic resonance imaging (MRI), use various algorithms to reconstruct key white matter tracts within the brain and have revealed the presence of lateralized tracts throughout development suggesting hemispheric specialization (Basser & Jones, 2002; Gong, Jiang, Zhu, Zang, He, et al., 2005; Gong, Jiang, Zhu, Zang, Wang, et al., 2005; Lebel & Beaulieu, 2009; Schmithorst et al., 2007; Thiebaut de Schotten et al., 2011).

Modern studies of neurological disorders are increasingly focusing on white matter connectomics—structural connections throughout the entire brain—to identify signatures of pathology (Fornito et al., 2015). In structural connectomics studies, the brain's white matter tracts are reconstructed using diffusion MRI and combined with an atlas to estimate structural connectivity patterns between different regions of interest (ROI). Multiple algorithms have been used to reconstruct these tracts, such as diffusion tensor models, more complex spherical deconvolution (CSD) models, and others, all having different strengths (Tournier et al., 2011). Specifically, the CSD model has been shown to be effective at resolving crossing fibers in areas

with more than one fiber population (Farquharson et al., 2013; Jeurissen et al., 2010) a challenge that is ubiquitous across the brain (Jeurissen et al., 2013). Using graph theory, structural connectivity of reconstructed tracts can be quantified across the entire brain or individual hemisphere, producing useful metrics characterizing complex network organization patterns (Fornito et al., 2015).

Graph theory is a mathematical interpretation of topology, or the way regions are connected, that was originally used in the planning of roadways in major cities (Biggs et al., 1986). Since the inception of graph theory in the late 1700s, the model has since been adapted to various applications, including understanding connectivity patterns in the brain. Such patterns may reveal how efficient certain neurological regions are by inferring connections that are directly connected to each other provide a more efficient means of communication compared to projecting through other additional regions (i.e., global efficiency) (Rubinov & Sporns, 2010). Further, one can infer that a region is important if many other regions are connected to that region (i.e., clustering coefficient [CC]), or if paths from other regions must project through a certain region to communicate with another part of the brain (i.e., betweenness centrality [BC]) (Rubinov & Sporns, 2010).

Studies examining structural connectivity patterns in childhood and adolescence have often suggested an increase during development in global efficiency, a metric that describes the average shortest path length to traverse from one region to another (Baum et al., 2017; Chen et al., 2013; Dennis et al., 2013; Dennis & Thompson, 2013; Hagmann et al., 2010; Hagmann et al., 2012; Huang et al., 2015; Khundrakpam et al., 2013; Tymofiyeva et al., 2014; Wierenga et al., 2016; Yap et al., 2011; Zhao et al., 2015). Further, an increase in network integration and concurrent decrease in network segregation is consistent with preclinical studies that show an evolution from local to global connections (Dennis et al., 2013; Hagmann et al., 2010; Yap et al., 2011). However, few studies have explicitly investigated hemispheric asymmetries in network properties in children and adolescents, and their results are slightly contradictory (Dennis et al., 2013; Zhong et al., 2017). Specifically, multiple studies investigating brain networks in adolescents and adults have shown hemispheric asymmetries in connectivity patterns, where the left hemisphere is more efficient than the right hemisphere (Caeyenberghs & Leemans, 2014; Dennis et al., 2013), however, others have shown the opposite (Zhong

TABLE 1 Image acquisition information

Dataset	No. of scans	B-value	No. of diffusion directions	No. of b_0 volumes	Voxel size	TR/TE
1	21	750	32	3	$0.86 \times 0.86 \times 2.2$	11.5/69.1
2	25	900	30	5	$0.86 \times 0.86 \times 2.2$	14.0/92.5
3	21	750	32	3	$0.86 \times 0.86 \times 2.2$	12.0/88.0
4	32	750	32	3	$0.86 \times 0.86 \times 2.2$	12.0/98.0
5	17	900	30	5	$0.86 \times 0.86 \times 2.2$	11.5/69.1
6	27	900	26	3	$0.86 \times 0.86 \times 2.2$	11.5/69.1
7	30	900	32	4	$0.86 \times 0.86 \times 2.2$	12.0/88.0
8	38	900	30	5	$0.95 \times 0.95 \times 2.2$	12.0/88.0

Note: This table outlines the imaging parameters of the diffusion MRI sequences that were used in this collaborative study. Abbreviations: TE, echo time (milliseconds); TR, repetition time (seconds).

et al., 2017). Contrasting hemispheric asymmetry results are also seen in the adult literature (Caeyenberghs & Leemans, 2014; Iturria-Medina et al., 2011). Since white matter properties are developing throughout childhood and adolescence, a more refined description of hemispheric trends is imperative to improve understanding of functional specialization and the impact of neurological diseases in pediatric populations. Also of interest, though less common in the literature, are network characteristics of more specific, functionally-based subnetworks as these may give additional insight into differing developmental trajectories that have implications for network analysis in various neurological diseases.

The current study used a single-site database of typically developing children who underwent MRI suitable for connectomic analyses. We characterized structural topological differences between the left and right hemispheres from childhood to young adulthood using established graph theory metrics (Rubinov & Sporns, 2010). Further, we investigated topological lateralization of various functionally-defined networks. We hypothesized that the left hemisphere would have higher global efficiency and hierarchical complexity (HC) compared to the right hemisphere, and that efficiency for both hemispheres would be associated with age.

2 | METHODS

2.1 | Population

The study included data from 211 typically developing participants from eight research studies who completed a research MRI at the Alberta Children's Hospital in Calgary, Alberta, Canada. Original consents from each study allowed for the secondary re-use of data. This collaborative study was approved by the University of Calgary Research Ethics Board. Inclusion criteria were (1) aged between 6 and 21 years, (2) no history of neuropsychiatric or developmental disorders through parent or self-report, or semi-structured interviews, (3) completion of a diffusion MRI with a b -value ~ 1000 s/mm² and ~ 32 diffusion directions, and (4) completion of a T1-weighted anatomical MRI. Participants were excluded if substantial head motion prevented processing of the MRI.

2.2 | Neuroimaging acquisition

All scans were acquired using the same 3T GE (Waukesha, WI) MR750w pediatric research scanner with a 32-channel head coil at the Alberta Children's Hospital's (ACH) Child and Adolescence Imaging Research (CAIR) program. Imaging parameters for each substudy are given in Table 1.

2.3 | Neuroimage processing

The image-processing pipeline is shown in Figure 1. Anatomical T1-weighted images were processed using statistical parametric mapping 12 (SPM12, <https://www.fil.ion.ucl.ac.uk/spm/software/spm12/>), which segmented brain tissue into gray matter, white matter, cerebrospinal fluid (CSF), bone, and air. A 5-tissue-type image was then created including gray matter, subcortical gray matter assessed by FSL's "FIRST," white matter, CSF, and a fifth optional image that was available but never used in this study. This 5-volume image defined the interface between white and gray matter, serving two purposes: first, it was the seed image used to generate whole-brain tractography, and second, it constricted the respective reconstructed tracts to only be contained in white-matter areas (Smith et al., 2012).

Diffusion scans were corrected for eddy currents and small motion using FSL's "eddy_correct." (Jenkinson et al., 2012) All scans were then visually assessed on the coronal and axial plane. To be included in the analysis, each scan required a minimum of 25 volumes not greatly affected by motion. Response functions were calculated for each individual using the "Tournier" algorithm. Whole brain tractography was then performed via MRtrix3's "tckgen" with the "iFOD2" algorithm extracting 1 M streamlines (Tournier et al., 2010). The "iFOD2" algorithm was preferentially used instead of the tensor model due to the CSD model's reliability and superior ability to resolve crossing fibers (Boukadi et al., 2019; Jeurissen et al., 2010; Newman et al., 2020; Tournier et al., 2010). Commands utilized optimized default settings as well as implemented anatomically constrained tractography (ACT) with the prior gray matter white matter interface image serving as the seed and cut-off images (Smith et al., 2012; Tournier et al., 2019). This

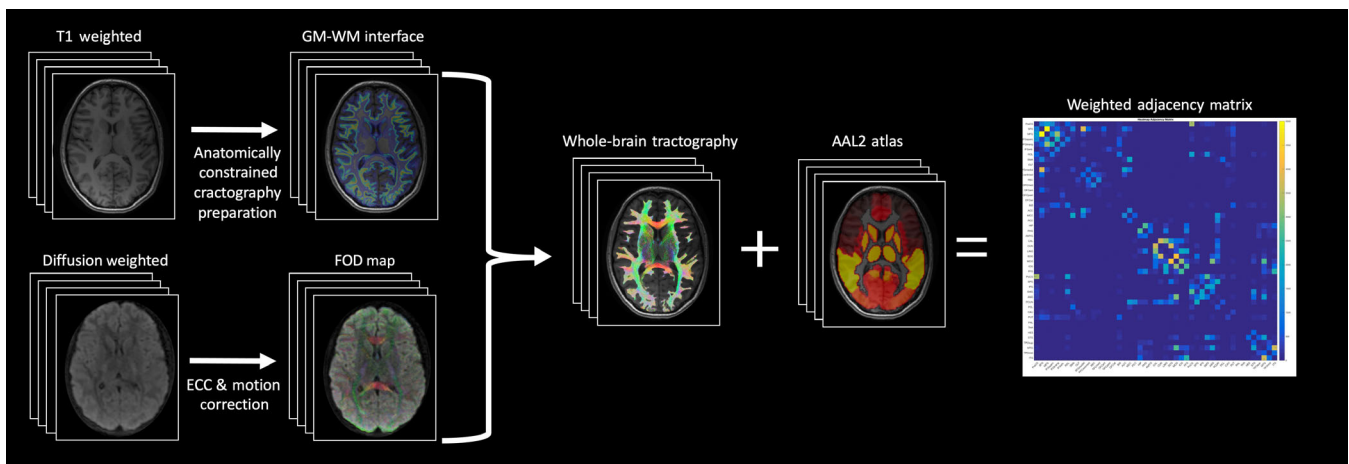


FIGURE 1 Displays the major processing steps to generate the structural connectome. Anatomical images were processed using statistical parametric mapping (SPM) and FSL. Diffusion images and adjacency matrix generation were processed using MRTrx3. AAL2, automated anatomical labelling 2 atlas; ECC, Eddy current correction; FOD, fiber orientation distributions; GM, gray matter; WM, white matter

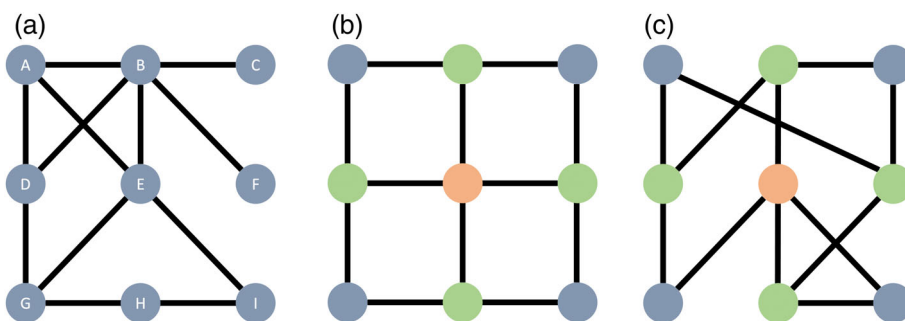


FIGURE 2 Is a graphic representation to help illustrate different graph theory metrics. Nodes are defined as the circles and the lines represent the edges that connect the nodes. Degree is defined as the number of nodes one node is connected to. For example, node H in Figure 2a has a degree of 3

reduced the presence of spurious streamlines and two authors additionally examined the color-coded, directional reconstruction of streamlines slice-by-slice independently assuring that streamline directionalities were appropriately anatomically representative.

2.4 | Structural connectome generation

The automated anatomical labelling 2 (AAL2) atlas, consisting of 120 brain regions covering the whole cortex and main subcortical structures, was used to define ROI (Rolls et al., 2015). The AAL2 atlas was first linearly then nonlinearly transformed into participant-space using FSL's "FLIRT" and "FNIRT," respectively (Jenkinson et al., 2012). The AAL2 atlas was then overlaid onto the whole-brain tracts to extract a measure of connectivity. A weighted connectivity measure was defined as the number of streamlines that enters/begins between each pair of ROIs. A number was generated based on every connection and ROI to generate a weighted, symmetrical adjacency matrix of 120×120 ROIs. In accordance with prior studies, cerebellar ROIs were excluded due to various imaging acquisitions not including the cerebellum consistently in the field of view (Craig et al., 2020). This left a 94×94 ROI matrix that was then split into left and right hemispheres for a pair of final weighted, symmetric adjacency matrices that were 47×47 ROIs in size. The weighted matrix underwent density-

based thresholding to remove the bottom 25% of potentially spurious reconstructed streamlines (Chapter 11 - *statistical Connectomics*, 2016; Erdős & Renyi, 1961).

2.5 | Graph theory outcomes

2.5.1 | General definitions

A node is a delineated brain region, represented by circles in Figure 2. For our analysis, we defined nodes as regions from the AAL template. An edge is what connects each node (i.e., reconstructed streamline count), represented as lines between circles in Figure 2. A path is any route of connections to get from one node to another within the network. Degree is the total number of other nodes that a given node is connected to. All metrics were generated using the Brain Connectivity Toolbox (Rubinov & Sporns, 2010).

2.5.2 | Global efficiency

Global efficiency (E_{glob}) is a global measure based on the notion that paths with fewer segments are more efficient (Rubinov & Sporns, 2010). For example, in Figure 2a, it would be more efficient to

travel from node A to I directly through E, rather than having to go through nodes D, G, and H. Here, the shortest path length from node A to node I is 2 (A-E-I), whereas the longest path length would be 4 (A-D-G-H-I). E_{glob} measures the average shortest path length for every node in the network. It may be energetically advantageous in the brain to have generally shorter path lengths as it may allow regions to communicate faster with one another.

2.5.3 | Hierarchical complexity

As the brain is inherently a complex structure, the global measure of HC attempts to quantify the complexity of connectivity within a topological area (Smith et al., 2019). In this metric, a network is more simple, and in turn less complex, if all nodes with the same degree are connected to other nodes with the same degree. For example, in Figure 2b, which would be considered an ordered (therefore less complex) network, all nodes with a degree of 2 (blue nodes) are connected to other nodes with a degree of 3 (green). Similarly, all nodes with a degree of 3 are connected to one node that has a degree of 4 (orange) and 2 nodes with a degree of 2. This would be contrasted with a more complex network, such as the one in Figure 2c, where while each node has the same degree as in Figure 2b, the nodes they are connected to appear to join with nodes of various degrees. For example, while the node with a degree of 4 (node C) in Figure 2b was connected to only nodes with a degree of 3, it is connected to nodes with a degree of 3 and 2 in Figure 2c. Higher complexity of brain structure/connections has been positively correlated with increased higher-level cognitive processing abilities (Smith, 2019).

2.5.4 | Clustering coefficient

Clustering coefficient assesses how connected a node's direct neighbors are to each other (Rubinov & Sporns, 2010). If two direct neighbors of a node are connected to each other, they would then create a closed triplet, such as the one between nodes A-B-E. The more connected neighbors are, the higher the CC. For example, in Figure 2a, node A would have a higher CC than node G. Here, node A has 2/3 potentially closed triplets (A-B-E and A-B-D), compared to node G, where no direct neighbors are connected to each other. Neurologically, a high CC may represent a situation where small networks may be present that work together on various tasks. CC is first calculated for each individual node and can also be averaged across larger regions, such as networks or hemispheres. Here, we used CC as an average across entire hemispheres and as an average of all nodes in various networks.

2.5.5 | Betweenness centrality

Betweenness centrality represents how "central" a node is by assessing how many connections go through a single node to get to other nodes within the network (Rubinov & Sporns, 2010). For example, in Figure 2a, node F has a low BC as no connections need to go through

node F to get to another node in the network, compared to node B, which would have a higher relative BC as both nodes C and F must go through node B to be connected to the rest of the network. Higher BC may represent the presence of hub nodes or a node where many connections come together. Like CC, an average of all nodes' BC can be used as an estimate of the hemisphere's overall tendency to have "central" nodes or can be used as a direct measure of how "central" a specific node is. Similar to CC, BC was used as an average of each hemisphere and various networks.

2.6 | Statistical analyses

2.6.1 | Demographic analysis

Shapiro-Wilk tests assessed distribution normality of age within each dataset separately. A nonparametric Kruskal-Wallis one-way analysis of variance (ANOVA) tested differences in participant age between datasets followed by Dwass-Steel-Critchlow-Fligner (DSCF) pairwise tests to identify which datasets differed from each other (correcting for multiple comparisons [MCs]). An independent test compared ages between participant groups who were scanned using a *b*-value of 750 versus 900 s/mm².

2.6.2 | Hemispheric analysis

A linear mixed effect model (LMEM) in Jamovi (<https://gamlj.github.io/>) was used to assess fixed effects of hemisphere, age, and sex on the respective graph theory metric (E_{glob} , HC, CC, and BC), with random effects of participant (to account for data in each hemisphere) and diffusion sequence. Interactions between the fixed effects were applied in the first model, before correction for MCs, and removed if they were not significant. Factors that showed significant relationships to graph theory metrics were further investigated using Wilcoxon signed-rank test or Spearman correlations where normality was first assessed by the Kolmogorov-Smirnov test. Bonferroni correction was used to correct for MCs.

2.6.3 | Network-wise analysis

Additional investigations assessing between-hemisphere differences in specific functionally-defined cortical networks were completed. Networks were defined in two steps. First, the automated anatomical labelling 2 atlas (AAL2) was overlaid on to the MNI152 brain template. Second, the CONN Network Cortical ROIs (HCP-ICA) were overlaid on top of the AAL2 atlas, defining intrinsic connectivity networks such as the sensorimotor, default mode, visual, salience, dorsal attention, and language networks (Whitfield-Gabrieli & Nieto-Castanon, 2012). Values within the AAL2 atlas that were in the same neurological space as the CONN Network Cortical ROIs were extracted, and defined the nodes considered to be a part of the respective network. Nodes from the AAL2 atlas that are in each network are given in Table 2.

TABLE 2 Defining major cortical networks

Network	AAL2 node left	AAL2 node right	AAL2 node names
Sensorimotor	1	2	Precentral gyrus
	15	16	Supplementary motor area
	61	62	Postcentral gyrus
Default mode	13	14	Rolandic operculum
	19	20	Superior frontal gyrus, medial
	55	56	Middle occipital gyrus
	69	70	Angular gyrus
	71	72	Precuneus
Visual	84	85	Superior temporal gyrus
	47	48	Calcarine fissure and surrounding cortex
	49	50	Cuneus
	51	52	Lingual gyrus
	53	54	Superior occipital gyrus
	57	58	Inferior occipital gyrus
Salience	93	94	Inferior temporal gyrus
	5	6	Middle frontal gyrus
	7	8	Inferior frontal gyrus, opercular part
	13	14	Rolandic operculum
	27	28	Anterior orbital gyrus
	33	34	Insula
	37	38	Middle cingulate gyrus and paracingulate gyri
67	68	Supramarginal gyrus	
Dorsal attention	3	4	Superior frontal gyrus, dorsolateral
	61	62	Postcentral gyrus
	63	64	Superior parietal gyrus
	65	66	Inferior parietal gyrus, excluding supramarginal and angular gyri
	67	68	Supramarginal gyrus
Language	9	10	Inferior frontal gyrus
	11	12	Inferior frontal gyrus pars orbitalis
	67	68	Supramarginal gyrus
	85	86	Superior temporal gyrus
	89	90	Middle temporal gyrus

Note: This table displays the various AAL2 nodes that were used to define various networks for the graph theory metrics.

Similar to the hemispheric analysis, a LMEM in Jamovi was used to investigate fixed effects of hemisphere, sex, and age, and random effects of participant and diffusion sequence, with the network graph theory metric (CC and BC) as the dependent variable. Post hoc analysis was identical to the hemispheric analysis.

3 | RESULTS

3.1 | Population

The initial sample consisted of 223 participants, but 12 were removed due to excessive head motion. The final sample consisted of

211 participants (mean 14.01 ± 3.26 years; range = 6.48–21.08 years; 51% female). Distributions of age and sex are shown in Figure S1. A total of 196 participants were right-handed (93%). Median age was the same for most datasets, except for slightly older participants in dataset 3 compared to datasets 1 ($p = .015$), 4 ($p < .01$), and 8 ($p < .01$) ($H = 38.9$, $p < .001$, Figure S1). Age and sex distributions were not different between the two groups using b -values of 750 versus 900 s/mm².

3.2 | Hemispheric analysis

Linear mixed effect model results are summarized in Table 3 and Figure 3. E_{glob} , HC, CC and BC all showed significant differences

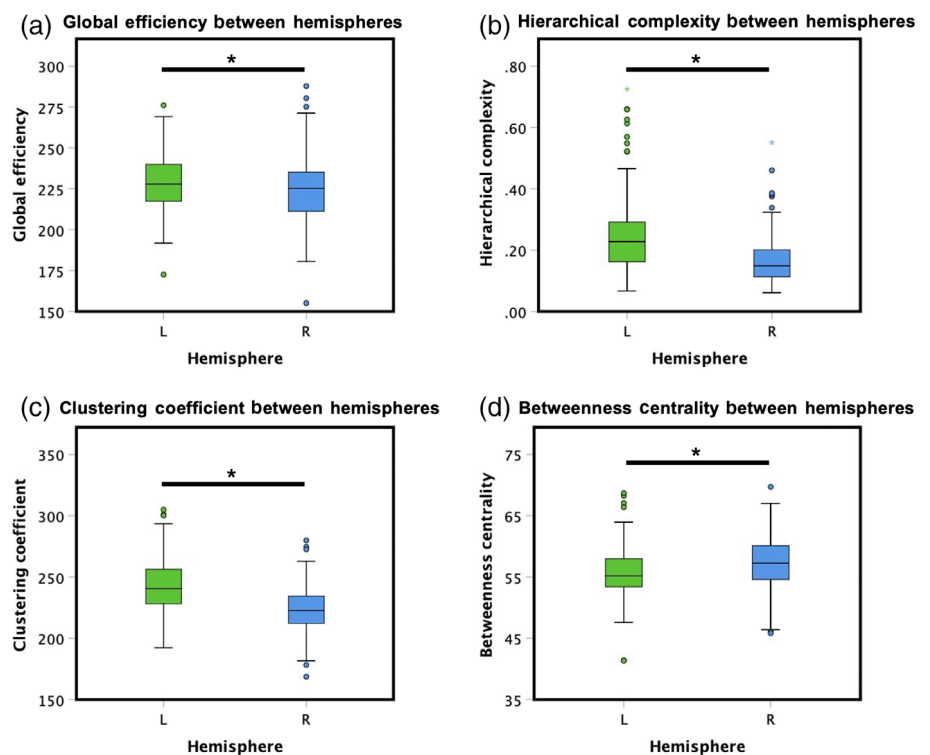
TABLE 3 Structural connectivity differences between hemispheres using graph theory.

Graph theory metric	R ² adjusted	Predictor	Estimates ± SE	Confidence interval	t statistic	p
Global efficiency	0.684	Hemisphere	−4.61 ± 1.04	−6.65 to −2.58	4.44	<.001***
		Sex	−3.40 ± 2.12	−0.76 to 7.56	1.60	.440
		Age	0.83 ± 0.34	0.16 to 1.50	2.44	.064
Hierarchical complexity	0.296	Hemisphere	−0.08 ± 0.01	−0.10 to −0.07	9.59	<.001***
		Sex	−0.01 ± 0.01	−0.02 to 0.01	0.59	.124
		Age	0.00 ± 0.00	−0.01 to 0.00	1.47	.576
		Sex × Age	0.01 ± 0.00	0.00 to 0.01	2.38	.072
Clustering coefficient	0.491	Hemisphere	−18.31 ± 1.48	−21.21 to −15.41	12.38	<.001***
		Sex	−0.35 ± 2.12	−3.81 to 4.51	0.16	.999
		Age	0.76 ± 0.34	0.10 to 1.42	2.24	.104
Betweenness centrality	0.187	Hemisphere	1.42 ± 0.38	0.68 to 2.15	3.77	<.001***
		Sex	−0.16 ± 0.44	−0.71 to 1.02	0.35	.999
		Age	0.15 ± 0.07	0.01 to 0.29	2.16	.128

Note: This table displays the results of the linear mixed effects model of the hemispheric analysis. All *p*-values have been corrected for multiple comparisons using the Bonferroni method.

****p* < .001.

FIGURE 3 Shows the relationships between various graph theory metrics and how they differ between the left and right hemisphere, where global efficiency, hierarchical complexity, clustering coefficient are higher in the left hemisphere and betweenness centrality is higher in the right hemisphere. Error bars represent the 95% confidence interval. L, left hemisphere; R, right hemisphere; **p* < .001



between hemispheres. E_{glob} , HC, and CC were higher in the left hemisphere compared to the right, and BC was higher in the right hemisphere. Age and sex were not related to any of the metrics. The interaction between sex and age for HC was nominally significant but did not survive Bonferroni correction.

3.3 | Network analysis

Results for the network analysis are given in Table 4. CC of the sensorimotor network was higher in the left than the right hemisphere (Figure 4a), whereas BC did not show any difference between

TABLE 4 Lateralization of major cortical networks using structural connectivity and graph theory.

Network	Metric	R ² adjusted	Predictor	Estimates ± SE	Confidence interval	Statistic	p
Sensorimotor	Clustering coefficient	0.342	Hemisphere	-5.93 ± 0.95	-7.80 to 4.06	6.22	<.001***
			Sex	-1.63 ± 1.28	-4.13 to 0.87	1.28	.406
			Age	0.48 ± 0.20	0.04 to 0.83	2.16	.064
	Betweenness centrality	0.276	Hemisphere	5.02 ± 3.59	-2.03 to 12.06	1.40	.328
			Sex	3.72 ± 4.17	-4.45 to 11.90	0.89	.746
			Age	0.581 ± 0.67	-0.74 to 1.90	0.86	.778
Default mode	Clustering coefficient	0.395	Hemisphere	-28.22 ± 2.35	-32.82 to -23.63	12.04	<.001***
			Sex	-0.59 ± 2.87	-6.20 to 5.02	0.21	.999
			Age	-0.733 ± 0.46	-1.63 to 0.17	1.60	.222
	Betweenness centrality	0.211	Hemisphere	-5.36 ± 2.60	-10.44 to -0.28	2.07	.080
			Sex	1.87 ± 3.08	-4.16 to 7.90	0.61	.999
			Age	0.35 ± 0.49	-0.62 to 1.31	0.70	.966
Visual	Clustering coefficient	0.425	Hemisphere	3.69 ± 3.20	-2.57 to 9.95	1.16	.498
			Sex	9.91 ± 4.63	0.84 to 18.99	2.14	.066
			Age	4.12 ± 0.73	2.69 to 5.56	5.63	<.001***
	Betweenness centrality	0.245	Hemisphere	-0.58 ± 2.10	-4.70 to 3.54	0.28	.999
			Sex	-5.77 ± 2.61	-10.90 to -0.65	2.21	.056
			Age	-0.30 ± 0.42	-1.12 to 0.52	0.72	.944
Salience	Clustering coefficient	0.388	Hemisphere	-11.89 ± 1.73	-15.28 to -8.50	6.87	<.001***
			Sex	0.73 ± 2.46	-4.10 to 5.55	0.30	.999
			Age	0.56 ± 0.39	-0.20 to 1.32	1.44	.302
	Betweenness centrality	0.213	Hemisphere	7.17 ± 1.55	4.14 to 10.20	4.64	<.001***
			Sex	-0.81 ± 1.85	-4.43 to 2.81	0.44	.999
			Age	0.54 ± 0.28	-0.02 to 1.09	1.90	.118
Dorsal attention	Clustering coefficient	0.441	Hemisphere	1.57 ± 2.17	-2.67 to 5.82	0.73	.936
			Sex	-1.61 ± 3.30	-8.08 to 4.86	0.49	.999
			Age	2.22 ± 0.52	1.19 to 3.25	4.24	<.001***
	Betweenness centrality	0.233	Hemisphere	-36.47 ± 11.21	-58.44 to -14.49	3.25	.002**
			Sex	-0.08 ± 2.94	-5.83 to 5.68	0.03	.999
			Age	0.01 ± 0.48	-0.91 to 0.94	0.03	.999
Hemisphere × Age			2.11 ± 0.78	0.59 to 3.63	2.71	.014*	
Language	Clustering coefficient	0.449	Hemisphere	-38.40 ± 2.73	-43.75 to -33.04	14.1	<.001***
			Sex	33.93 ± 15.21	4.13 to 63.73	2.23	.054
			Age	-0.44 ± 0.55	-1.52 to 0.64	0.80	.854
			Sex × Age	-2.70 ± 1.06	-4.78 to -0.63	2.55	.022*
	Betweenness centrality	0.357	Hemisphere	-3.52 ± 2.41	-8.24 to 1.19	1.46	.290
			Sex	6.60 ± 2.97	0.78 to 12.41	2.22	.054
			Age	0.56 ± 0.48	-0.39 to 1.49	1.15	.506

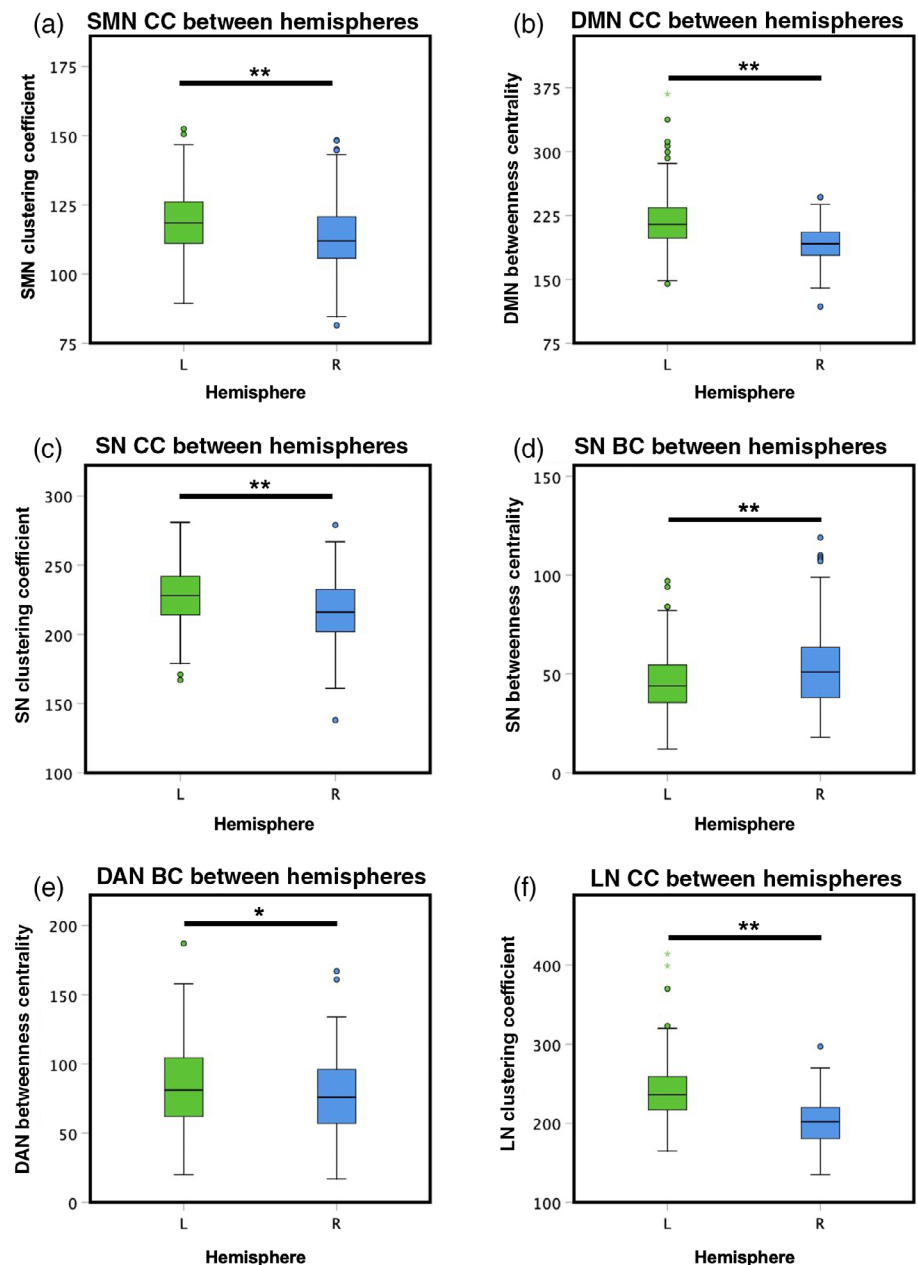
Note: This table displays the linear mixed effects model results from the network analysis. All *p*-values have been corrected for multiple comparisons using the Bonferroni method.

p* < .05. *p* < .01. ****p* < .001.

hemispheres. Age and sex were not significant factors for either metric. CC of the default mode network was significantly higher in the left hemisphere compared to the right (Figure 4b), whereas BC was not different between hemispheres. Age and sex were not significant factors for either metric. CC and BC of the visual network did not differ

between hemispheres. Age was positively related with CC but not BC. Sex was not a significant factor for CC or BC. CC of the salience network was higher in the left hemisphere compared to the right (Figure 4c), whereas BC was higher in the right hemisphere compared to the left (Figure 4d). Age and sex were not significant factors for

FIGURE 4 Shows different networks being compared between the left and right hemispheres. Error bars represent the 95% confidence interval. $**p < .001$; $*p = .00$. BC, betweenness centrality; CC, clustering coefficient; DAN, dorsal attention network; DMN, default mode network; L, left hemisphere; LN, language network; R, right hemisphere; SMN, sensorimotor network; SN, salience network



either metric. CC of the dorsal attention network did not differ between hemispheres, but BC was higher in the left hemisphere (Figure 4e). CC was positively associated with age but not with sex. A significant interaction between hemisphere and age revealed that BC of the dorsal attention network decreased in the left hemisphere at older ages, with the opposite relationship with age in the right hemisphere. CC of the language network was higher in the left hemisphere compared to the right (Figure 4f), but the hemispheres did not differ in BC. The interaction between sex and age was significant, such that CC of the language network was positively related to age in females but negatively related to age in males. BC had no significant relation to age or sex in the language network.

4 | DISCUSSION

The present study describes structural connectivity differences between the left and right hemisphere in a sample of children, adolescents, and young adults. Our findings reveal topological differences between hemispheres in typically developing populations for multiple brain networks. Age and sex were not related to most outcomes, suggesting that structural topology may be relatively stable throughout school-aged development compared to other macro- and microscale measures and may only change during later adolescence or early adulthood. Using the combination of structural diffusion MRI techniques with anatomical parcellations to generate graph theory

representations of brain networks is a promising tool to better understand lateralization during neurodevelopment.

4.1 | Hemispheric-level analysis

At the hemispheric level, we found that global efficiency was higher in the left hemisphere compared to the right, confirming our original hypothesis. This finding aligns with two prior studies in samples of different ages: the first was a mixed sample of adults and children ($N = 102 < 18$ years old) (Dennis et al., 2013) and the second was a large cohort of 346 adults (Caeyenberghs & Leemans, 2014). This hemispheric asymmetry may be associated with cortical volume as both cerebral cortex and white matter volume are, on average, larger in the right hemisphere, potentially resulting in more long range and less efficient connections (Giedd et al., 1996), though recent research suggests that intracranial volume is not associated with graph theory metrics (Wierenga et al., 2016). Since our sample was mostly right handed (93%), it seems more likely that the “dominant”, classically left-sided networks such as the language, sensorimotor, or other networks may have exhibited more efficient connections compared to the right hemisphere, manifesting as higher global efficiency in the left (Corballis, 2014). This finding contrasts with Zhong et al. (2017), who found that the right hemisphere was more efficient (Zhong et al., 2017). One possible explanation for this discrepancy is the slight age difference between the populations, where Zhong et al. (2017) included participants between the ages of 11–26 years, compared to the younger group in our current study that included children as young as 6 years of age (6–21 years). Differences in statistical methodology and network resolution may also underlie these disparate findings. In the Zhong study, participant age was used a between-group factor rather than a continuous covariate and connectivity matrices contained 512×512 ROIs (higher resolution) compared to 94×94 in the present study. Other reasons for such discrepancies between these quite similar, well-powered studies are still somewhat unclear but also reflect inconsistencies reported in the adult literature (Caeyenberghs & Leemans, 2014; Iturria-Medina et al., 2011). Further studies may assist in clarifying these differing findings.

Interestingly, global efficiency was not related to age in either hemisphere, suggesting that lateralization did not differ across the age range of our cohort (6–21 years). In contrast, most research has shown that global efficiency of the whole brain has a positive relationship with age (Baum et al., 2017; Chen et al., 2013; Dennis et al., 2013; Hagmann et al., 2010; Huang et al., 2015; Khundrakpam et al., 2013; Wierenga et al., 2016; Yap et al., 2011; Zhao et al., 2015). The current findings contrast with those of Dennis et al. (2013), who found that the efficiency of the left hemisphere network increased with age while the right decreased. Participant sample differences may explain our different findings, as Dennis et al. (2013) included individuals between the ages of 12–30 years while almost half of our sample was younger than 13 years. We have likely captured different developmental time points, and one explanation could be that efficiency does not increase until late adolescence and early adulthood

(>20), ages we did not comprehensively sample (Chen et al., 2013; Dennis et al., 2013). It could also be that developmental trajectories are not linear. We used a linear mixed model for exploring associations with age, and more complex, nonlinear patterns may exist (Baum et al., 2017; Chen et al., 2013), something we were not optimized to detect despite sufficient statistical power. The calculation of the average metrics within a given hemisphere also may obscure trends present within more specific networks developing at different rates. For example, when investigating CC, which is related to efficiency, the dorsal attention network shows a strong positive relationship with age in the left hemisphere (Figure 4e), whereas some networks do not relate to age at all. Similar to Dennis et al. (2013), we did not find sex differences in global efficiency within either hemisphere. These findings are consistent with white-matter microstructure metrics in similarly aged populations (Lebel & Beaulieu, 2011).

For HC, left hemisphere topology was more complex compared to the right hemisphere. This means that, on average, regions with similar connectivity patterns tend to connect in a more ordered fashion, rather than a more complex one, in the right hemisphere compared to the left. In the absence of prior studies investigating lateralization of HC at any age, we can only speculate why the left hemisphere is more complex, or less ordered, than the right. A potential explanation could be that our mostly right-handed population has a “dominant” left hemisphere. Increased use of the left hemisphere to control the dominant hand, for example may result in a more complex connectome than a simpler, more ordered “nondominant” hemisphere. Further, we have previously shown that HC was higher in controls compared to children who have survived strokes near birth (Craig et al., 2020).

The CC was higher in the left hemisphere compared to the right, whereas BC was higher in the right hemisphere compared to the left. These findings suggest that the neighbors of nodes are more likely to be connected in the left hemisphere, whereas the right hemisphere tends to have more nodes that serve as a central hub compared to the left hemisphere. The higher CC in the left hemisphere adds converging evidence to the hypothesis that the left hemisphere is more connected than the right and, in turn, is more efficient. This finding of higher left hemisphere CC is supported by previous findings in a sample of adolescents and young adults (Dennis et al., 2013). A higher BC and lower complexity score may be associated. As a more ordered network, the right hemisphere potentially has more critical nodes that serve as a “pitstop” to other connections.

4.2 | Network-level analysis

We also investigated lateralization of topological outcomes in six networks. The sensorimotor, default mode, salience, and language networks showed a leftward asymmetry of the CC, suggesting that the neighbors of the nodes within these networks are more likely to be connected in the left hemisphere than the right. For the sensorimotor, default mode, and language networks, higher clustering could represent a dominance of connectivity of the left hemisphere, as our

population was mainly right-handed. A left-lateralized clustering of these networks is supported by similar findings in functional MRI studies and other diffusion studies across the lifespan (Agcaoglu et al., 2015; Banks et al., 2018; Vassal et al., 2016). Whether this increase in clustering is caused by activity-dependent neuroplasticity or itself drives dominance is yet to be determined. Absence of relationships with age suggests that this lateralization may already be developed by age six. While age can often be used as a proxy for neurodevelopment, this may not hold true when investigating topological neurodevelopment (Lebel et al., 2017). However, this may be important when investigating neurodiverse populations (Craig et al., 2020).

Betweenness centrality was only lateralized in the salience and dorsal attention networks. The salience network had higher BC in the right hemisphere, while it was higher in the dorsal attention network in the left hemisphere. The rightward laterality of BC in the salience network is confirmed in various fMRI studies potentially highlighting an overlap of structural and functional connectivity (Seeley et al., 2007; Zhang et al., 2019). Previous studies have shown that the dorsal attention network is thought to be symmetrically organized (Vossel et al., 2014); thus, our finding of a leftward asymmetry in BC is novel. Further, BC appears to decrease in the left hemisphere with age but increases in the right hemisphere with age. This could potentially suggest that the right hemisphere develops more critical nodes compared to the left hemisphere.

4.3 | Implications

An understanding of typical, healthy structural connectivity provides a baseline that can be used to help reveal how the brain develops in response to injuries or neurologic conditions. We provide evidence of strong and consistent differences in laterality of structural connectivity across childhood and adolescence. This lateralization may play a critical role in cognitive specialization and should be further investigated in clinical populations. To our knowledge, only a few studies have investigated lateralization of structural topology between hemispheres and have generated contradictory answers suggesting that further investigations would be helpful in elucidating this disparity (Dennis et al., 2013; Iturria-Medina et al., 2011; Zhong et al., 2017). Perhaps the most interesting finding across our analyses is the lack of relationship between topological outcomes and age, which contrasts with a vast literature demonstrating microstructural changes across white-matter development throughout childhood and adolescence (Lebel et al., 2017). Specifically, the results suggest that, perhaps during early development, the underlying properties of white matter in those tracts are changing in ways that do not alter structural topology. Therefore, while the brain's microstructure may be changing, its connectivity patterns during this time may be static. As prior studies have revealed topological changes at different stages of later stages of the lifespan, this may reflect a complex, nonlinear relationship across the entirety of the lifespan (Dennis et al., 2013; Zhong et al., 2017). Topological organization or reorganization may be a valuable tool to further predict and understand disease (Fornito et al., 2015).

4.4 | Limitations

Although this study draws on participants from a single site and scanner, the data were collected from eight different research projects as part of a larger collaboration. To account for small differences in b -values (750 vs. 900 s/mm²) and number of diffusion directions (26–32), we used sequence as a random effect in our model. Across all models, sequence accounted for <5.3% of the variance of the model, with an average of 2.7%. Interestingly, recent evidence shows that large variations in b -values (1200 vs. 3000 s/mm²) and number of diffusion directions (30 vs. 60) still leads to relatively consistent tractography results and only small (<5%) variations in FA values (Schilling et al., 2021). We do concede that there are differences in methodology between the two studies that should be considered, such that Schilling et al. (2021) used fractional anisotropy and a tract of interest approach rather than our current methods of using streamline count and graph theory. Nonetheless it is encouraging to see relatively small variations in results with the use of somewhat different diffusion parameters. Despite these mitigation strategies, there remains the possibility that the use of slightly different diffusion parameters added additional variability to our dataset. Due to the lack of consistent acquisitions of reverse phase-encoded diffusion sequences for all participants, EPI distortion correction was not performed, potentially causing a slight geometric mismatch between the anatomical and diffusion sequences. We did not use spherical-deconvolution informed filtering of tractograms (SIFT), which may have improved the accuracy of the reconstructed connectomes. It has been suggested that the use of rigorous tools like SIFT2 (Smith et al., 2015a) or COMMIT2 (Schiavi et al., 2020) is important to reduce possible tracking biases and make resulting streamline count biologically meaningful (Calamante, 2019; Jones et al., 2013), more in-line with underlying fiber density. We also could have reconstructed a greater number of streamlines (100 vs. 1 M), a difference that has been shown to increase accuracy and reduce variability of resulting connectomes when combined with algorithms such as SIFT2 (Smith et al., 2015b). Given the additional significant computational costs of reconstructing 100 M streamlines, 1 M was used here. Future endeavors will include these powerful tools combined with 100 M streamline connectomes.

Many different graph theory metrics can be used to assess brain topology. Although we did not investigate all graph theory metrics, we attempted to use a subset of them that account for unique topological features (Smith, 2019). Further, many approaches can be used to investigate adjacency matrices that generate graph theory metrics – we elected to pursue a weighted matrix that may be more relevant to clinical populations. Even with the small number of graph theory outcomes, the stringent Bonferroni correction used to adjust our findings for MCs may have resulted in some false negatives (type 2 error). However, we can be confident that the remaining significant results are unlikely to be false positives (type 1 error). We used an atlas developed from resting state functional MRI networks to define our ROI, which were subsequently used to investigate structural

connectivity. Although this may appear to be uncommon, a recent study has highlighted consistencies between structural and functional networks (Osmanlıoğlu et al., 2019). Functional networks are well-established in the literature and have been repeatedly validated, therefore functionally-defined connectomics assessing lateralization may provide synergistic information to our study. In addition, developmental trajectories of specific functional networks have been shown to differ in the time-period between early childhood and early adulthood (Betzel et al., 2014; Rubia, 2013) and investigating similarly-defined structural networks may shed light on such differing developmental processes. Finally, although the nodes that were assigned within each network are limited in number, they may also be structurally connected to other nodes that are outside of the assigned network. Therefore, we postulate that this method can still inform on laterality, sex, and age-related associations in such networks.

5 | CONCLUSION

In our investigation of topological lateralization of the brain in children, adolescents, and young adults, we found strong, consistent differences between hemispheres. Surprisingly, age did not play a significant role in our cross-sectional study, highlighting that while microstructural changes likely occur in this developmental period, topological changes may be static in early development and in turn represent a more complex, nonlinear trajectory throughout all courses of development. The utilization of topological outcomes using structural connectivity is a potentially advantageous tool for understanding the development of brain connectivity and laterality.

ACKNOWLEDGMENTS

The authors would like to thank Mary Kate Dichoso for the retrieval and organization of all neuroimaging files. Brandon T. Craig was supported by a Vanier Canadian Graduate Scholarship. Brian L. Brooks acknowledges salary funding from the Canadian Institutes for Health Research (CIHR) Embedded Clinician Researcher Salary Award. Funding for scan acquisition was supported through CIHR, Alberta Children's Hospital Foundation, and Alberta Health Services.

CONFLICT OF INTEREST

Brian L. Brooks receives royalties for the sales of the Pediatric Forensic Neuropsychology textbook (2012, Oxford University Press) and three pediatric neuropsychological tests (Child and Adolescent Memory Profile [ChAMP, Sherman and Brooks, 2015, PAR Inc.], Memory Validity Profile [MVP, Sherman and Brooks, 2015, PAR Inc.], and Multidimensional Everyday Memory Ratings for Youth [MEMRY, Sherman and Brooks, 2017, PAR Inc.]). Brian L. Brooks has previously received in-kind support (free test credits) from the publisher of the computerized cognitive test (CNS Vital Signs, Chapel Hill, North Carolina). Keith O. Yeates is supported by the Ronald and Irene Ward Chair in Pediatric Brain Injury from the Alberta Children's Hospital Foundation.

DATA AVAILABILITY STATEMENT

A dataset with deidentified participant data and a data dictionary will be made available upon reasonable request from any qualified investigator, subject to a signed data access agreement.

ORCID

Brandon T. Craig  <https://orcid.org/0000-0003-1222-1284>

Catherine Lebel  <https://orcid.org/0000-0002-0344-4032>

Helen L. Carlson  <https://orcid.org/0000-0002-5788-0542>

REFERENCES

- Agcaoglu, O., Miller, R., Mayer, A. R., Hugdahl, K., & Calhoun, V. D. (2015). Lateralization of resting state networks and relationship to age and gender. *NeuroImage*, 104, 310–325.
- Banks, S. J., Zhuang, X., Bayram, E., Bird, C., Cordes, D., Caldwell, J. Z., & Cummings, J. L. (2018). Default mode network lateralization and memory in healthy aging and Alzheimer's disease. *Journal of Alzheimer's Disease*, 66, 1223–1234.
- Basser, P. J., & Jones, D. K. (2002). Diffusion-tensor MRI: Theory, experimental design and data analysis - a technical review. *NMR in Biomedicine*, 15, 456–467.
- Baum, G. L., Ciric, R., Roalf, D. R., Betzel, R. F., Moore, T. M., Shinohara, R. T., Kahn, A. E., Vandekar, S. N., Rupert, P. E., Quarmley, M., Cook, P. A., Elliott, M. A., Ruparel, K., Gur, R. E., Gur, R. C., Bassett, D. S., & Satterthwaite, T. D. (2017). Modular segregation of structural brain networks supports the development of executive function in youth. *Current Biology*, 27, 1561–1572 e8.
- Betzel, R. F., Byrge, L., He, Y., Goñi, J., Zuo, X. N., & Sporns, O. (2014). Changes in structural and functional connectivity among resting-state networks across the human lifespan. *NeuroImage*, 102(Pt 2), 345–357.
- Biggs, N., Lloyd, E., & Wilson, R. (1986). *Graph theory*, 1736–1936. Oxford University Press.
- Boukadi, M., Marcotte, K., Bedetti, C., Houde, J. C., Desautels, A., Deslauriers-Gauthier, S., Chapleau, M., Boré, A., Descoteaux, M., & Brambati, S. M. (2019). Test-retest reliability of diffusion measures extracted along white matter language fiber bundles using HARDI-based tractography. *Frontiers in Neuroscience*, 12, 1055.
- Broca, P. (1861). Remarques sur le siège de la faculté du langage articulé, suivies d'une observation d'aphémie (perte de la parole). *Bulletin et Memoires de la Societe anatomique de Paris*, 6, 330–357.
- Caeyenberghs, K., & Leemans, A. (2014). Hemispheric lateralization of topological organization in structural brain networks. *Human Brain Mapping*, 35, 4944–4957.
- Calamante, F. (2019). The seven deadly sins of measuring brain structural connectivity using diffusion MRI streamlines fibre-tracking. *Diagnostics (Basel)*, 9, E115.
- Fornito, A., Zalesky, A., & Bullmore, E. T. (Eds.) (2016). Chapter 11 - Statistical connectomics. In *Fundamentals of brain network analysis* (pp. 383–419). Academic Press. <https://doi.org/10.1016/B978-0-12-407908-3.00011-X>
- Chen, Z., Liu, M., Gross, D. W., & Beaulieu, C. (2013). Graph theoretical analysis of developmental patterns of the white matter network. *Frontiers in Human Neuroscience*, 7, 716.
- Corballis, M. C. (2014). Left brain, right brain: Facts and fantasies. *PLoS Biology*, 12, e1001767.
- Craig, B. T., Hilderley, A., Kinney-Lang, E., Long, X., Carlson, H. L., & Kirton, A. (2020). Developmental neuroplasticity of the white matter connectome in children with perinatal stroke. *Neurology*, 95, e2476–e2486.
- Dennis, E. L., Jahanshad, N., McMahon, K. L., De Zubicaray, G. I., Martin, N. G., Hickie, I. B., Toga, A. W., Wright, M. J., & Thompson, P. M. (2013). Development of brain structural connectivity

- between ages 12 and 30: A 4-tesla diffusion imaging study in 439 adolescents and adults. *NeuroImage*, 64, 671–684.
- Dennis, E. L., & Thompson, P. M. (2013). Mapping connectivity in the developing brain. *International Journal of Developmental Neuroscience*, 31, 525–542.
- Erdős, P., & Renyi, A. (1961). On the strength of connectedness of a random graph. *Acta Mathematica Hungarica*, 12, 261–267.
- Farquharson, S., Tournier, J. D., Calamante, F., Fابيني, G., Schneider-Kolsky, M., Jackson, G. D., & Connelly, A. (2013). White matter fiber tractography: Why we need to move beyond DTI. *Journal of Neurosurgery*, 118, 1367–1377.
- Fornito, A., Zalesky, A., & Breakspear, M. (2015). The connectomics of brain disorders. *Nature Reviews Neuroscience*, 16, 159–172.
- Giedd, J. N., Snell, J. W., Lange, N., Rajapakse, J. C., Casey, B. J., Kozuch, P. L., Vaituzis, A. C., Vauss, Y. C., Hamburger, S. D., Kaysen, D., & Rapoport, J. L. (1996). Quantitative magnetic resonance imaging of human brain development: Ages 4–18. *Cerebral Cortex*, 6, 551–560.
- Gong, G., Jiang, T., Zhu, C., Zang, Y., He, Y., Xie, S., & Xiao, J. (2005). Side and handedness effects on the cingulum from diffusion tensor imaging. *Neuroreport*, 16, 1701–1705.
- Gong, G., Jiang, T., Zhu, C., Zang, Y., Wang, F., Xie, S., Xiao, J., & Guo, X. (2005). Asymmetry analysis of cingulum based on scale-invariant parameterization by diffusion tensor imaging. *Human Brain Mapping*, 24, 92–98.
- Hagmann, P., Grant, P. E., & Fair, D. A. (2012). MR connectomics: A conceptual framework for studying the developing brain. *Frontiers in Systems Neuroscience*, 6, 43.
- Hagmann, P., Sporns, O., Madan, N., Cammoun, L., Pienaar, R., Wedeen, V. J., Meuli, R., Thiran, J. P., & Grant, P. E. (2010). White matter maturation reshapes structural connectivity in the late developing human brain. *Proceedings of the National Academy of Sciences of the United States of America*, 107, 19067–19072.
- Huang, H., Shu, N., Mishra, V., Jeon, T., Chalak, L., Wang, Z. J., Rollins, N., Gong, G., Cheng, H., Peng, Y., Dong, Q., & He, Y. (2015). Development of human brain structural networks through infancy and childhood. *Cerebral Cortex*, 25, 1389–1404.
- Iturria-Medina, Y., Pérez Fernández, A., Morris, D. M., Canales-Rodríguez, E. J., Haroon, H. A., García Pentón, L., Augath, M., Galán García, L., Logothetis, N., Parker, G. J. M., & Melie-García, L. (2011). Brain hemispheric structural efficiency and interconnectivity rightward asymmetry in human and nonhuman primates. *Cerebral Cortex*, 21, 56–67.
- Jenkinson, M., Beckmann, C. F., Behrens, T. E. J., Woolrich, M. W., & Smith, S. M. (2012). FSL. *NeuroImage*, 62, 782–790.
- Jeurissen, B., Leemans, A., Tournier, J.-D., Jones, D. K., & Sijbers, J. (2010). Estimating the number of fiber orientations in diffusion MRI voxels: A constrained spherical deconvolution study. In *International Society for Magnetic Resonance in Medicine (ISMRM)* (Vol. 573).
- Jeurissen, B., Leemans, A., Tournier, J.-D., Jones, D. K., & Sijbers, J. (2013). Investigating the prevalence of complex fiber configurations in white matter tissue with diffusion magnetic resonance imaging. *Human Brain Mapping*, 34, 2747–2766.
- Jones, D. K., Knösche, T. R., & Turner, R. (2013). White matter integrity, fiber count, and other fallacies: The do's and don'ts of diffusion MRI. *NeuroImage*, 73, 239–254.
- Khundrakpam, B. S., Reid, A., Brauer, J., Carbonell, F., Lewis, J., Ameis, S., Karama, S., Lee, J., Chen, Z., das, S., Evans, A. C., Brain Development Cooperative Group, Ball, W. S., Byars, A. W., Schapiro, M., Bommer, W., Carr, A., German, A., Dunn, S., ... O'Neill, J. (2013). Developmental changes in organization of structural brain networks. *Cerebral Cortex*, 23, 2072–2085.
- Lebel, C., & Beaulieu, C. (2009). Lateralization of the arcuate fasciculus from childhood to adulthood and its relation to cognitive abilities in children. *Human Brain Mapping*, 30, 3563–3573.
- Lebel, C., & Beaulieu, C. (2011). Longitudinal development of human brain wiring continues from childhood into adulthood. *The Journal of Neuroscience*, 31, 10937–10947.
- Lebel, C., Treit, S., & Beaulieu, C. (2017). A review of diffusion MRI of typical white matter development from early childhood to young adulthood. *NMR in Biomedicine*, 32, e3778. <https://doi.org/10.1002/nbm.3778>
- Newman, B. T., Dholander, T., Reynier, K. A., Panzer, M. B., & Druzgal, T. J. (2020). Test-retest reliability and long-term stability of three-tissue constrained spherical deconvolution methods for analyzing diffusion MRI data. *Magnetic Resonance in Medicine*, 84, 2161–2173.
- Osmanlioglu, Y., Tunç, B., Parker, D., Elliott, M. A., Baum, G. L., Ciric, R., Satterthwaite, T. D., Gur, R. E., Gur, R. C., & Verma, R. (2019). System-level matching of structural and functional connectomes in the human brain. *NeuroImage*, 199, 93–104.
- Rolls, E. T., Joliot, M., & Tzourio-Mazoyer, N. (2015). Implementation of a new parcellation of the orbitofrontal cortex in the automated anatomical labeling atlas. *NeuroImage*, 122, 1–5.
- Rubia, K. (2013). Functional brain imaging across development. *European Child & Adolescent Psychiatry*, 22, 719–731.
- Rubinov, M., & Sporns, O. (2010). Complex network measures of brain connectivity: Uses and interpretations. *NeuroImage*, 52, 1059–1069.
- Schiavi, S., Ocampo-Pineda, M., Barakovic, M., Petit, L., Descoteaux, M., Thiran, J. P., & Daducci, A. (2020). A new method for accurate in vivo mapping of human brain connections using microstructural and anatomical information. *Science Advances*, 6, eaba8245.
- Schilling, K. G., Tax, C. M. W., Rheault, F., Hansen, C., Yang, Q., Yeh, F. C., Cai, L., Anderson, A. W., & Landman, B. A. (2021). Fiber tractography bundle segmentation depends on scanner effects, vendor effects, acquisition resolution, diffusion sampling scheme, diffusion sensitization, and bundle segmentation workflow. *NeuroImage*, 242, 118451.
- Schmithorst, V. J., Holland, S. K., & Dardzinski, B. J. (2007). Developmental differences in white matter architecture between boys and girls. *Human Brain Mapping*, 29, 696–710.
- Seeley, W. W., Menon, V., Schatzberg, A. F., Keller, J., Glover, G. H., Kenna, H., Reiss, A. L., & Greicius, M. D. (2007). Dissociable intrinsic connectivity networks for salience processing and executive control. *The Journal of Neuroscience*, 27, 2349–2356.
- Smith, K., Bastin, M. E., Cox, S. R., Valdés Hernández, M. C., Wiseman, S., Escudero, J., & Sudlow, C. (2019). Hierarchical complexity of the adult human structural connectome. *NeuroImage*, 191, 205–215.
- Smith, K. M. (2019). On neighbourhood degree sequences of complex networks. *Scientific Reports*, 9, 8340.
- Smith, R. E., Tournier, J.-D., Calamante, F., & Connelly, A. (2012). Anatomically-constrained tractography: Improved diffusion MRI streamlines tractography through effective use of anatomical information. *NeuroImage*, 62, 1924–1938.
- Smith, R. E., Tournier, J.-D., Calamante, F., & Connelly, A. (2015a). SIFT2: Enabling dense quantitative assessment of brain white matter connectivity using streamlines tractography. *NeuroImage*, 119, 338–351.
- Smith, R. E., Tournier, J.-D., Calamante, F., & Connelly, A. (2015b). The effects of SIFT on the reproducibility and biological accuracy of the structural connectome. *NeuroImage*, 104, 253–265.
- Stone, S. P., Wilson, B., Wroot, A., Halligan, P. W., Lange, L. S., Marshall, J. C., & Greenwood, R. J. (1991). The assessment of visuospatial neglect after acute stroke. *Journal of Neurology, Neurosurgery, and Psychiatry*, 54, 345–350.
- Thiebaut de Schotten, M., ffytche, D. H., Bizzi, A., Dell'Acqua, F., Allin, M., Walshe, M., Murray, R., Williams, S. C., Murphy, D. G. M., & Catani, M. (2011). Atlasing location, asymmetry and inter-subject variability of white matter tracts in the human brain with MR diffusion tractography. *NeuroImage*, 54, 49–59.
- Toga, A. W., & Thompson, P. M. (2003). Mapping brain asymmetry. *Nature Reviews Neuroscience*, 4, 37–48.

- Tournier, J. D., Calamante, F., & Connelly, A. (2010). Improved probabilistic streamlines tractography by 2nd order integration over fibre orientation distributions. *Proceedings of the International Society for Magnetic Resonance Medicine* (Vol. 1670). New Jersey, USA: John Wiley & Sons, Inc.
- Tournier, J. D., Mori, S., & Leemans, A. (2011). Diffusion tensor imaging and beyond. *Magnetic Resonance in Medicine*, *65*, 1532–1556.
- Tournier, J.-D., Smith, R., Raffelt, D., Tabbara, R., Dhollander, T., Pietsch, M., Christiaens, D., Jeurissen, B., Yeh, C. H., & Connelly, A. (2019). MRtrix3: A fast, flexible and open software framework for medical image processing and visualisation. *NeuroImage*, *202*, 116137.
- Tymofiyeva, O., Hess, C. P., Xu, D., & Barkovich, A. J. (2014). Structural MRI connectome in development: Challenges of the changing brain. *The British Journal of Radiology*, *87*, 20140086.
- Vassal, F., Schneider, F., Boutet, C., Jean, B., Sontheimer, A., & Lemaire, J. J. (2016). Combined DTI tractography and functional MRI study of the language connectome in healthy volunteers: Extensive mapping of white matter fascicles and cortical activations. *PLoS One*, *11*, e0152614.
- Vossel, S., Geng, J. J., & Fink, G. R. (2014). Dorsal and ventral attention systems. *The Neuroscientist*, *20*, 150–159.
- Wernicke, C. (1874). *Der aphasische symptomcomplex*. Springer-Verlag.
- Whitfield-Gabrieli, S., & Nieto-Castanon, A. (2012). Conn: A functional connectivity toolbox for correlated and anticorrelated brain networks. *Brain Connectivity*, *2*, 125–141.
- Wierenga, L. M., Van den Heuvel, M. P., Van Dijk, S., Rijks, Y., De Reus, M. A., & Durston, S. (2016). The development of brain network architecture. *Human Brain Mapping*, *37*, 717–729.
- Yap, P.-T., Fan, Y., Chen, Y., Gilmore, J. H., Lin, W., & Shen, D. (2011). Development trends of white matter connectivity in the first years of life. *PLoS One*, *6*, e24678.
- Zhang, Y., Suo, X., Ding, H., Liang, M., Yu, C., & Qin, W. (2019). Structural connectivity profile supports laterality of the salience network. *Human Brain Mapping*, *40*, 5242–5255.
- Zhao, T., Cao, M., Niu, H., Zuo, X. N., Evans, A., He, Y., Dong, Q., & Shu, N. (2015). Age-related changes in the topological organization of the white matter structural connectome across the human lifespan. *Human Brain Mapping*, *36*, 3777–3792.
- Zhong, S., He, Y., Shu, H., & Gong, G. (2017). Developmental changes in topological asymmetry between hemispheric brain white matter networks from adolescence to young adulthood. *Cerebral Cortex*, *27*, 2560–2570.
- Zhou, D., Lebel, C., Evans, A., & Beaulieu, C. (2013). Cortical thickness asymmetry from childhood to older adulthood. *NeuroImage*, *83*, 66–74.

SUPPORTING INFORMATION

Additional supporting information can be found online in the Supporting Information section at the end of this article.

How to cite this article: Craig, B. T., Geeraert, B., Kinney-Lang, E., Hilderley, A. J., Yeates, K. O., Kirton, A., Noel, M., MacMaster, F. P., Bray, S., Barlow, K. M., Brooks, B. L., Lebel, C., & Carlson, H. L. (2023). Structural brain network lateralization across childhood and adolescence. *Human Brain Mapping*, *44*(4), 1711–1724. <https://doi.org/10.1002/hbm.26169>